By Air by SEA

Evan B. Davis, Boeing Commercial Airplanes, Seattle, Washington

Transitioning Statistical Energy Analysis (SEA) based design and analysis tools from research to production support is a confidence building process. The Boeing confidence building process is a model, test and check process. The size and complexity of the test articles used in the confidence building exercise range from simple transmission loss structures to a fully fitted 767 laboratory test vehicle. The SEA model sizes have increased from a few wave-field subsystems for transmission loss models to thousands of wave-field subsystems for the fully furnished fuselage section model. Verification of the transfer function measured with well-controlled laboratory sources builds confidence in the application of the prediction process but unfortunately solves only part of the problem. Aeroacoustic and engine related fluctuating pressure fields drive the structure and must be represented in order to predict absolute noise levels in the airplane during flight. Boeing has an in-house source-model development program using a combination of semi-empirical models and measured external pressure field data to drive the structural-acoustic models.

The goal of Statistical Energy Analysis (SEA) modeling is to estimate cabin noise levels in flight in the mid to high frequencies. For double aisle airplanes, the frequency range where SEA modeling is easily justified is in the range of 500 to 20,000 Hz. Due to lack of a practical alternative, SEA calculations for airplane cabin models are run down to 100 Hz with the understanding that the variation about the mean value estimates will increase at the lower frequencies. SEA is based on the assumption of energy transfer between resonant modes, so frequency limitations are best viewed as a requirement for the subsystems to have many modes. In other words, the dimensions of the system understudy should be large relative to the characteristic wavelength in that system. In this article a four window/frame bay model length is used, with an approximately length of 2.5 m, which is long relative to the acoustic wavelength at 1000 Hz, but short relative to an acoustic wavelength at 50 Hz.

Uncertainty in the predictions and measurements are unavoidable, however the sources of uncertainty can be understood and bounded with good engineering practice. Uncertainty in the predictions can be viewed as three separate problems with different approaches to reducing the uncertainty. There is an uncertainty in the input power, which is a major concern for the in-flight noise predictions, there is an uncertainty in the transfer functions, which can be refined using laboratory tests, and there is an uncertainty in the definition of the SEA model and its subsystems.

Initial In-Flight Noise Predictions

The following in-flight cabin noise prediction study is an example of the confidence building process of model, test and check. The test data in this case are the typical in-flight survey data Boeing collects for the first of the model flights and for airplane customers to meet contractual obligations. On some flight tests, sound intensity data are collected, which give a bit more insight on where the energy is coming into the cabin. The intensity data are collected in areas much smaller than the size of the subsystems used in the initial models. Although the total energy reaching the cabin is correct, the distribution of the energy flow, as indicted by sound intensity surveys, shows discrepancies that require model refinement.

The initial study was an attempt to predict interior noise levels in the forward cabin of a wide range of airplanes. The airplanes were represented with 37 subsystems and the input power was derived from a turbulent boundary layer (TBL) model. The TBL model was developed in-house and is based on the work of B. M. Efimtsov. A review paper by Graham[1] states that the Efimtsov model is the best of the current Corcos-type TBL models for predicting the fluctuating pressure spectra, convection speed and spatial correlation scale lengths from a large database of flight and wind tunnel measurements. The external field properties used in conjunction with a joint acceptance calculation provides an input power to the SEA model. Any error in either the external field description or the joint acceptance calculation will show up as a one-for-one, dB-for-dB error in the cabin SPL. If an airplane fuselage skin gage is such that the bending wave speed is very similar to the convection speed of the turbulent boundary layer, then there will be a very high sensitivity to small changes in the convection speed or the skin gage. The turbulent boundary layer pressure fluctuations are very high and have a very short correlation scale; fortunately the conventional aluminum airplane structure is poorly matched to accept energy form the TBL source.

SEA models were built and compared on a 1/3 octave band basis for 737, 757, 767 and 777 airplanes. These airplanes have slightly different cruise Mach numbers and flight altitudes, and the measurements used in the comparisons were at different body stations. In other words, each model was driven by a TBL model appropriate to the given body station and flight condition. All of the comparisons are forward of the wing so as to avoid the need for an engine exhaust plume noise model. Air conditioning on and off data were used to estimate the air conditioning system contribution to cabin noise (if any) and was added as an internal noise source to the airplane cabins that had measurable air conditioning noise components.

The prediction of the space average sound pressure levels differed from the measured data in a random fashion across the airplanes' models (Figure 1). The absolute predicted noise levels were within 5 dB on a 1/3-octave band basis. The Efimtsov turbulent boundary layer pressure fluctuations are a curve fit through data with a ±5 dB spread. The variation in the cabin space average models may simply be a reflection of the variation in the external pressure field. More likely, the differences are a combination of the external field not being exactly represented and simplifications in the representation of the airplane and trim structures. The limited number of SEA subsystems requires that the subsystems be defined in terms of effective properties. For example, the isolation mounts between the sidewall panels were represented with a single effective coupling loss factor.

The uncorrected 737 SEA model prediction is also presented as an example of the power of modeling a number of systems (airplanes) with the same techniques to build confidence in the modeling techniques. The difference was in the understanding of the definition of a 'spring' in AutoSEA.™ The isolators were intended to be represented by an axial spring. In AutoSEA™ an isolator is defined in general terms by a 6×6 complex matrix; in all the AutoSEA™ models the axial spring had the same values but the other impedances differed. Most modelers set the non-axial spring constants to the same value as the axial values, the 737 modeler did not. The body of evidence suggests the 737 model representation was not as good as the representation used by the other modelers.

A significantly more refined model was built for the 767 airplane. The number of subsystems has been increased from 37 to 327 subsystems. There is now a one-to-one correspondence between the physical subsystems and the SEA subsystems. A noise control engineer can now communicate with the design teams modifying the treatment package and assessing changes in the treatment. The graphical user interface gives an indica-

Based on a paper presented at NOISE-CON 2004, National Congress on Noise Control Engineering, Baltimore, MD, July 2004.

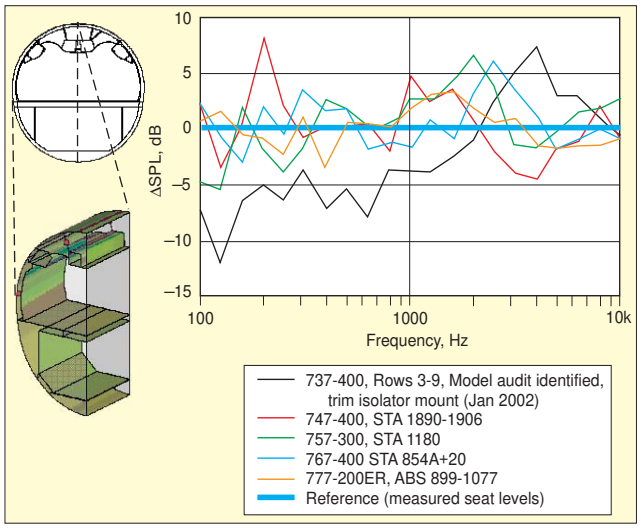

Figure 1. Difference between first generation SEA predicted model and space averaged measured cabin sound pressure levels (TBL & ECS). Compliance flight conditions at 35,000 ft, December 2001 model status.

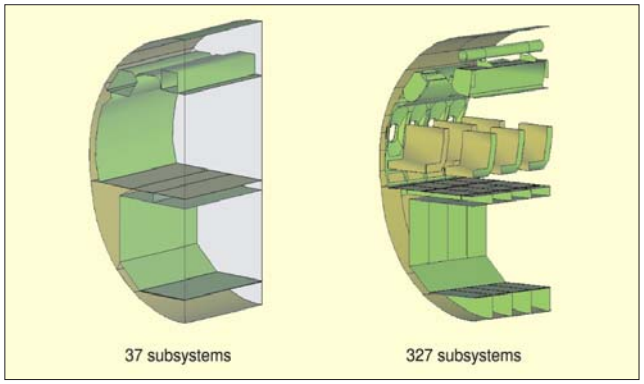

Figure 2. First and second generation SEA models.

tion of the increased detail in the refined model (Figure 2).

The AutoSEA™ code used defines subsystems as physical systems such as a plate, therefore the AutoSEA™ plate subsystem represents many wave types; each wave type is a traditional SEA subsystem. The AutoSEA plate subsystem is composed of flexural, axial and shear wave traditional SEA subsystems. The SEA matrix used internally in AutoSEA™ is larger than the AutoSEA™ subsystem count would suggest.

The in-flight sound intensity data adds detail in the confidence building process of model, test and check. The initial cabin sound pressure level predictions were within 5 dB of the flight data based on the space average cabin sound pressure levels. The refined model does not significantly improve the simpler estimate (Figure 3). However, the resolution of the balance of the sound power contribution from the various surfaces to the cabin has significantly improved. For example, the sidewall system's contribution to the total power input to the cabin is shown in Figure 4.

The sidewall input power is computed for all the subsystems included in the pictures. In the first generation SEA model, the power input is due to the trim panel, the mass-law across the sidewall trim panel and the air-return grill acting as a leak. The second-generation SEA model explicably models the windows, the air return grill, the sidewall sub panels, and the individual isolation mounts so local sound intensity survey data can be directly compared on the basis of these smaller features in the noise control package. There are known significant differences in the sound intensity levels over the sidewall trim system. The first generation SEA model does not have the detail for comparison with the flight data sets that the second generation SEA model does. Behind the trim system are the fiberglass thermal-acoustic insulation blankets that are modeled by the Delaney

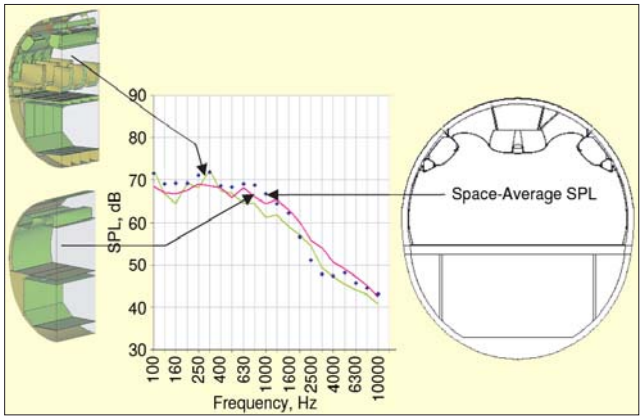

Figure 3. Comparison of first and second generation SEA models and space averaged cabin sound pressure levels due to TBL source + ECS component (Seat Row 10).

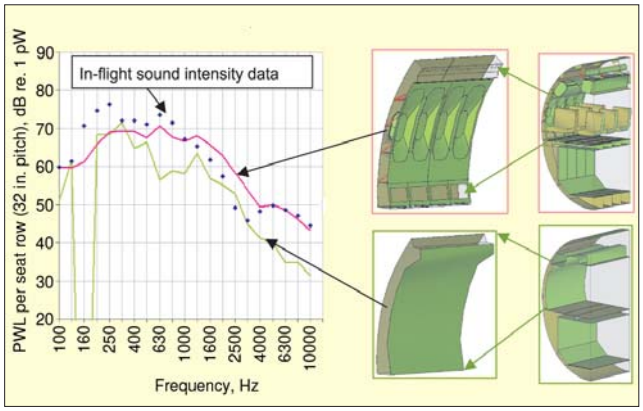

Figure 4. Data comparison of first and second generation SEA models of sound power input to cabin from sidewall paths (Seat Row 10).

and Bazley[2] algorithms.

The above comparisons are clouded as to whether they are dominated by input power differences or path differences. The uncertainty of the input power can be avoided, or at least greatly reduced, in a laboratory setting. The confidence building process of model, test and check now moves into the laboratory.

SEA Model Validation

The model validation and confidence building process of model, test and check work benefits from the use of controlled power inputs and the time available to make detailed surveys of the subsystem responses under specified loading conditions in the laboratory. The noise engineering laboratory in Seattle, WA houses the Interior Noise Test Facility (INTF). The INTF is a large reverberation room, anechoic chamber test suite sized to do full size fuselage testing (Figure 5). Between the anechoic and reverberation rooms is an approximately 4 × 4 m test window. The large test window can support a number of test articles including a production 757 sidewall section and a 757 crown section. The crown section is a uniform structure used for transmission loss tests similar to those used in architectural acoustics. The sidewall section is fitted with a production trim system including the floor, a space below the floor, trim panels, windows and stow-bin systems. The 757 test articles have been used to verify the SEA predictions of transmission loss and noise control system performance.

The 767 fuselage section is 11 frame bays in length and is closed off by acoustical bulkheads. The INTF-767 fuselage fits into the INTF reverberation room taking up approximately one third of the reverberation room's volume. A reverberant sound field excited by four independent speaker channels generates a space averaged 1/3 octave band level of 100 dB in the reverberation room for diffuse sound field excitations. The INTF-767 is moved to the anechoic chamber for shaker driven tests

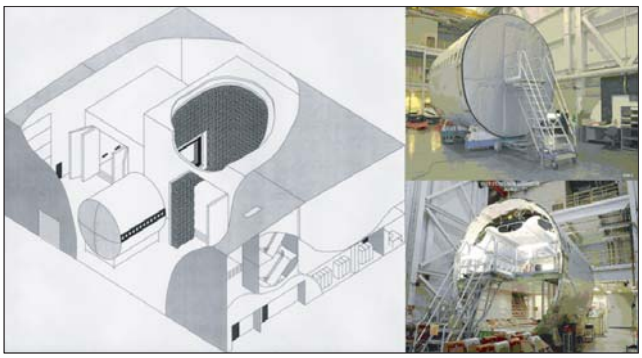

Figure 5. Interior Noise Test Facility (INTF) and 767 fuselage section.

and modal analysis tests. The INTF-767 is a recovered 767-200 airplane structure fitted with the latest 767-400 interior system. At this time, testing has been completed on the 767 fuselage and model updating is in progress. Modal analysis data will be used to refine the FEM models and energy transfer functions will be used to update the SEA models.

Noise reduction measurements of the differences in the space average SPL in the reverberation room and the INTF-767 fuselage compare well, as do the relative levels moving from a panel driven by a shaker to the interior of the fuselage. Look for future reports on this work.

Noise Control and SEA Energy Flow Paths

Noise control is based on identifying and then reducing energy flow paths. In order to design efficient noise control systems, the dominant energy flow paths through a complex structural acoustic system must be identified. Statistical Energy Analysis (SEA) and Finite Element Analysis (FEA) models are formulated to produce end-to-end transfer functions with little insight into the path the energy has taken to get from one point to the other. Energy-flow paths can be identified and the relative strengths of these paths computed from the SEA coupling loss factor matrix.

Two path-identification techniques are examined. The first is the back tracing of energy from receiver to source and the second is Craik's[3] coupling to total loss factor product ratio.

The back tracing of energy from receiver to source is based on looking at the power flows into subsystems starting with the receiver subsystem. The power input spectra of the receiver subsystem is examined and the dominant input power source identified. The dominant input subsystem now plays the role of the receiver and the input power spectrum for this intermediate subsystem is examined and the dominant input power source to this intermediate subsystem identified. The process of dominant input power source identification is repeated until a subsystem with a direct input power is reached. The dominant power paths are likely to be different for different frequency ranges.

Once a path has been identified, noise control treatments can be considered. Changing something in the dominant path will 'rebalance' the energy paths and the back tracing of energy from receiver to source process will begin again with the new model. Changing something in the original dominant path has no guarantee of reducing the response at the receiver position.

The process of back tracing energy from receiver to source is very labor intensive, because it requires examining the model one source at a time, and requires a lot of decision making in the ranking of input power contributions. The inevitable problem in this approach is the case where the input power spectra to any given subsystem shows that a number of power inputs of similar levels contribute so that a single dominant path cannot be identified. If the power inputs are similar at any point in the model, the path analysis must branch and follow the many parallel branches, greatly increasing the number of paths to be examined.

The advantages of back tracing energy from receiver to source is that most of the secondary paths will be excluded from analysis and the noise control design package will work on the critical path, acknowledging that the critical path or paths can and will change as the noise control solution is developed. The design of the noise control solution should employ the design of experiment's approach if multiple equally contributing paths are identified.

In SEA, a matrix of coupling loss factors describes the interaction of all coupled subsystems. The path the energy travels from source to receiver is not obvious from the coupling loss factor matrix. Craik has shown that the number of energy paths between any given source-receiver pair is infinite if the SEA model has more that two subsystems. The number of energy paths is infinite because energy can flow though each subsystem an infinite number of times on its way to the receiver. This is not unlike using image source models to represent reflections in room acoustics. An infinite number of image sources are required to model the room exactly. Fortunately, coupling and damping losses occur as energy moves across one subsystem to the next; the longer and the more convoluted the path, the more inefficient that path is at transporting energy from the source to the receiver. The number of energy flow paths that need to be screened is therefore finite. The analogy in the image source reflection models is that the order of the reflections is limited and the contributions of the higher order reflections can be neglected with little impact to the model.

Craik has developed a path definition that is computed from the SEA loss factor matrix. The path relates the power applied to subsystem a to the energy state of a receiver subsystem z. The path can be understood to be an energy ratio between the source and receiver subsystems.

The energy contribution from subsystem a to the receiver subsystem z through a specific path is

$$E_Z = \frac{\Pi_a}{\omega}\frac{\eta_{ab}\eta_{bc}\eta_{cd}\cdots\eta_{yz}}{\eta_a\eta_b\eta_c\cdots\eta_z}$$

The coupling loss factors used in the numerator are the off diagonal terms of the SEA loss-factor matrix. The denominator is the product of the subsystem total loss factors, the diagonal of the SEA loss factor matrix. The total loss factor is the sum of the subsystem damping loss factor and the coupling loss factors.

$$\eta_a = \eta_{aa} + \sum_{j\neq a}\eta_{aj}$$

The energy ratio between the source subsystem a and the receiver subsystem z can be computed by substituting the energy level of the source system into the path function generating a non-dimensional expression.

$$\frac{E_Z}{E_a} = \frac{\eta_{ab}\eta_{bc}\eta_{cd}\cdots\eta_{yz}}{\eta_b\eta_c\cdots\eta_z}$$

The energy of the source subsystem a is determined by its input power and total loss factor.

$$E_a = \frac{\Pi_a}{\omega\eta_a}$$

It needs to be understood that the subsystems (wave groups) can be used multiple times as energy moves through the system. Energy cycling through a group of subsystems would have a form

$$E_Z = \frac{\Pi_a}{\omega}\frac{\eta_{ab}\eta_{bc}\eta_{cd}\cdots}{\eta_a\eta_b\eta_c\cdots}\left(\frac{\eta_{mn}\eta_{no}\eta_{op}\cdots\eta_{uv}}{\eta_m\eta_n\eta_o\cdots\eta_v}\right)^N\frac{\cdots\eta_{yz}}{\cdots\eta_z}$$

Here N represents the number of time energy cycles though the loop and there can be multiple loops in any given path. The total loss factor, being the sum of the damping loss factors and coupling loss factors, guarantees that the longer the path, the lower the contribution to the final energy state. Energy taking the looped path is likely to contribute less energy to the receiver subsystem than the single-pass paths under the assumption that the coupling loss factors are of similar magnitudes.

In a large SEA model, many of the subsystems are typically

locally connected since subsystems are only connected to their immediate neighbors. The local connectivity greatly reduces the number of available non-zero energy transmission paths to explore.

The coupling loss factor matrix is available to the user in the AutoSEA™ software. An algorithm could be used to compute all of the possible paths through a given order. If subsystems are not connected in the SEA model, then the coupling loss factor for the pair is zero so one would expect a lot of path combinations that would yield no energy contribution to the receiver. Mechanically computing and then ranking all possible paths is a large computational job. More intelligent path identification and assessment algorithms are needed.

Uncertainty in the Path Equation

All prediction equations are subject to uncertainties in their estimates. There are two primary sources of uncertainty. The first source of uncertainty is rooted in the assumptions made to create a mathematical model. Some of these modeling assumptions are based on physical arguments, some on mathematical expediencies. The question of how well the mathematical model represents the 'real' world will be overlooked and the second source of uncertainty will be explored.

The second source of uncertainty is, given a fixed mathematical model, how well can one 'know' the input parameters? Most of the input parameters are determined from measurements – lengths, masses, etc. All measurements have some degree of uncertainty. Any 'paper' design can only be built to within given manufacturing tolerances. Therefore, even in the design stage, all parameters will have some uncertainty associated with them.

The uncertainty in any prediction equation can be expressed mathematically as a function of the uncertainty of the parameter and the sensitivity of the prediction equation to that parameter. Given a prediction equation

$$Y = F(x_1, x_2, x_3, \ldots x_n)$$

The general uncertainty estimate can, under certain assumptions, be expresses as the following function of the parameter uncertainties.

$$U_Y = \sqrt{\sum_{n=1}^{N}\left(U_{x_n}\frac{\partial F}{\partial x_n}\right)^2}$$

The general uncertainty equation can be executed analytically for many mathematical relationships or computed numerically if the mathematical functions do not lend themselves to simple expressions.

Craik's path analysis equation is in the mathematical form of a power law. Power law prediction equations are relativity common and fortunately the uncertainty estimate for a power law prediction equation is easy to compute.

A power law prediction equation has the general form

$$Y = x_1^a \times x_2^b \times x_3^c \ldots \times x_n^z$$

The uncertainty estimate for a power law prediction equation has the form,

$$\left(\frac{U_Y}{Y}\right)^2 = a^2\left(\frac{U_{x_1}}{x_1}\right)^2 + b^2\left(\frac{U_{x_2}}{x_2}\right)^2 + c^2\left(\frac{U_{x_3}}{x_3}\right)^2 + \ldots + z^2\left(\frac{U_{x_n}}{x_n}\right)^2$$

Craik's' path analysis equation is a power law expression and the uncertainty estimates are,

$$E_Z = \frac{\Pi_a}{\omega}\frac{\eta_{ab}\eta_{bc}\eta_{cd}\ldots\eta_{yz}}{\eta_a\eta_b\eta_c\ldots\eta_z}$$

$$\left(\frac{U_{E_Z}}{E_Z}\right)^2 = \left(\frac{U_{\Pi_a}}{\Pi_a}\right)^2 + \left(\frac{U_{\eta_a}}{\eta_a}\right)^2 + \left(\frac{U_{\eta_{ab}}}{\eta_{ab}}\right)^2 + \left(\frac{U_{\eta_b}}{\eta_b}\right)^2 + \left(\frac{U_{\eta_{bc}}}{\eta_{bc}}\right)^2 \ldots + \left(\frac{U_{\eta_{yz}}}{\eta_{yz}}\right)^2 + \left(\frac{U_{\eta_z}}{\eta_z}\right)^2$$

In the uncertainty expression the analysis frequency variable is assigned and therefore assumed to have no uncertainty associated with it.

The type of loss factor can be used to rearrange the uncertainty equation into three parts. The first term is the uncertainty in the input power. The next group of terms is related to the uncertainty in the total loss factors and the third term is due to the uncertainty in the coupling loss factors.

$$\left(\frac{U_{E_Z}}{E_Z}\right)^2 = \left(\frac{U_{\Pi_a}}{\Pi_a}\right)^2 + \left\{\left(\frac{U_{\eta_a}}{\eta_a}\right)^2 + \left(\frac{U_{\eta_b}}{\eta_b}\right)^2 \ldots + \left(\frac{U_{\eta_z}}{\eta_z}\right)^2\right\} + \left\{\left(\frac{U_{\eta_{ab}}}{\eta_{ab}}\right)^2 + \left(\frac{U_{\eta_{bc}}}{\eta_{bc}}\right)^2 \ldots + \left(\frac{U_{\eta_{yz}}}{\eta_{yz}}\right)^2\right\}$$

Coleman and Steele[4] suggest seeding the uncertainty estimator to understand the limitations of the model and its predictive power. All of the damping-loss and coupling-loss factors' uncertainties contribute to the total uncertainty estimate. If the uncertainty expression is seeded with uniform uncertainty estimates, coupling-loss, and damping-loss factors, one concludes that the longer the path, the more uncertainty there is in the energy contribution estimate to the receiver subsystem. The uncertainty estimate increases with the number of subsystems in the path, each subsystem contributing equally under the uniform parameter uncertainty estimate. A two subsystem path would have two total loss factor terms and one coupling loss factor term. A five subsystem path would have five total loss factors and four coupling loss factors contributing to the uncertainty estimate. The increased uncertainty of the long paths is in large part offset by the decreasing contribution to the receiver system's total energy via the long paths.

Observe that the uncertainties in loss factors of the source and receiver subsystems have no special role in determining the uncertainty in a given path. However, all paths that connect the source subsystem to the receiver subsystem will include the damping loss factors of the source and receiver subsystems. This gives the receiver and source subsystem damping-loss factors special leverage in model refinements. Note that the input-power uncertainty plays a role similar to the source or receiver subsystem's damping loss factor in determining the overall uncertainty in a multi-path SEA model.

SEA Paths Discussion

The SEA model has an infinite number of paths from a driven subsystem to a receiving subsystem. From a noise-control perspective, only the shorter, better coupled paths are of interest and warrant attention in a model refinement effort. However, as the short, easily reduced paths are addressed, another (generally larger) set of once secondary paths will need to be addressed. In time the whole model will need to be refined to correctly account for the roles of the many paths that contribute to the energy flow from one system to another. In a mature design there will be no simple solutions to gain significant changes in the receiver noise levels and a multi-dimensional optimization process will be required to get the last few dB out of the system. In that optimization study, physical constraints (e.g., those needed to transfer static loads through isolated connection points or the reluctance to add mass or complexity or cost) will ultimately limit the noise reduction potential of any system. In the airplane business the use of mass, which can be effectively used to significantly reduce energy transmission, has an adverse impact on airplane range and load capacity.

Conclusion

Forward cabin space-averaged sound pressure level (SPL) predictions using statistical energy analysis (SEA), structural acoustic models and a semi-empirical, turbulent boundary layer, external fluctuating pressure field model matched one third octave measured in-flight SPLs to within 5 dB. Refining the model changed the energy distribution paths but did not have a significant impact on the aircraft cabin noise level predictions.

Noise control work is based on the identification of energy flow paths and their reduction. At Boeing, path model refinements will be pursued with testing in the INTF 767 fuselage test section. The definition of an SEA energy path has been addressed and Craik's algorithm for computing the significance of a given path has been outlined as has a method for computing the uncertainty in an SEA path based on the work of Coleman and Steele. Automation of SEA path identification and ranking would be a significant improvement over the manual methods being used today. SEA will continue to be developed as a tool for the design of complex noise control systems using a confidence building model, test and check process.

Acknowledgments

The author would like to acknowledge the members of the SEA user team (at the time that the data in this article were created), Andrew Fung, Adam Weston, Hugh Poling, Mark Gmerek, Ashnapreet Nagi, Balakrishna Thanedar and Erik West. The SEA user team is tasked with advancing the modeling capabilities through peer reviews, organized seminars and training sessions. The current team is company wide and has a dynamic membership with many more members than those listed here.

References

1. Graham, W. R., "A Comparison of Models for the Wavenumber-Frequency Spectrum of Turbulent Boundary Layer Pressures," *Journal of Sound and Vibration*, Volume 206, Issue 4, 2, p 541-565. 1997.
2. Delany, M. E. and Bazley, E. N., "Acoustical Properties of Fibrous Absorbent Materials," *Applied Acoustics* (3), p 105-116. 1970.
3. Craik, R. J. M., "Sound Transmission Paths thought Statistical Energy Analysis Models," *Applied Acoustics* (30), p 45-55, 1990.
4. Coleman, H. W. and Steele, W. G., *Experimentation and Uncertainty Analysis for Engineers*, 2nd ed., John Wiley & sons, New York, NY 1999.

Appendix 1 — Overview of SEA

Statistical Energy Analysis (SEA) can be viewed as a statement of the conservation of energy and a hypothesis on how energy flows between connected systems.

SEA Power balance equations start with a power balance of a control volume or subsystem

$$\Pi_{in} = \Pi_{out}$$

The power loss from the control volume can either be dissipated in the control volume or transferred to other control volumes.

$$\Pi_{out} = \Pi_{diss} + \Pi_{others}^{out}$$

The power dissipated in a control volume can be expressed in terms of the energy state of the control volume E_s and a damping loss factor η_s and a characteristic radian frequency ω.

$$\Pi_{diss} = \omega\eta_s E_s$$

The power transfer from one control volume to another can be expressed in terms of the energy state of the control volume E_s and a coupling loss factor η_{sr} and a characteristic radian frequency ω. The systems are considered to be linear in that all energy in a frequency band stays in that frequency band. Nonlinear systems can transfer energy between frequencies. Energy transfer between frequencies is not accounted for in the following equation.

$$\Pi_{others}^{out} = \omega\eta_{sr}E_s$$

The power loss by a control volume can be stated as the sum of the power dissipated in the control volume by damping and the power transfer from the control volume to all other control volumes to which it is connected.

$$\Pi_{out} = \Pi_{diss} + \Pi_{others}^{out} = \omega\eta_s E_s + \sum \omega\eta_{sr}E_s$$

Coupling loss factor indices indicate source control volume and receiving control volume.

The power flowing into the control volume can either be applied directly in the control volume or transferred from the other control volumes.

$$\Pi_{in} = \Pi_{direct} + \Pi_{others}^{in}$$

The power transferred into the control volume is simply the power lost from other control volumes that are connected to control volume of interest. The power loss has been stated in terms of the control volume energy of the source volume.

$$\Pi_{others}^{in} = \sum \omega\eta_{rs}E_r$$

The power balance on the control volume of interest can now be expressed in terms of damping and coupling loss factors and the energy states of the other connected control volumes.

$$\Pi_{direct} + \Pi_{others}^{in} = \Pi_{diss} + \Pi_{others}^{out}$$

$$\Pi_{direct} + \sum \omega\eta_{rs}E_r = \omega\eta_s E_s + \sum \omega\eta_{sr}E_s$$

This equation can be restated in a form that is more useful for engineering purposes, from which the control volume energy states can be estimated. The energy states are related to engineering variables such as stress, velocities and pressures.

$$\Pi_{direct} = \omega\left(\eta_s + \sum \eta_{sr}\right)E_s - \omega\sum \eta_{rs}E_r$$

The equation can be written for every control volume leading to a family of simultaneous equations that can be written in standard matrix from.

$$\begin{bmatrix}\Pi_1\\ \Pi_2\\ \Pi_3\\ \cdots\\ \Pi_r\end{bmatrix} = \omega\begin{bmatrix}\eta_{11} & -\eta_{12} & -\eta_{13} & \cdots & -\eta_{1r}\\ -\eta_{21} & \eta_{22} & -\eta_{23} & \cdots & -\eta_{2r}\\ -\eta_{31} & -\eta_{32} & \eta_{33} & \cdots & -\eta_{3r}\\ \cdots & \cdots & \cdots & \cdots & \cdots\\ -\eta_{r1} & -\eta_{r2} & -\eta_{r3} & \cdots & \eta_{rr}\end{bmatrix}\begin{bmatrix}E_1\\ E_2\\ E_3\\ \cdots\\ E_r\end{bmatrix}$$

The diagonal terms of the matrix have the form of the damping loss factor of the control volume plus the sum of all the coupling loss factors.

$$\eta_{ss} = \eta_s + \sum_{r=1}^{N_{subsystems}} \eta_{sr}$$

This matrix represents the power balance equations for the various control volumes.

Appendix 2 — Experimental Determination of Damping and Coupling Loss Factors

The power balance equations give us an experimental method for determining the coupling loss factors and damping loss factor of our control volumes. These experiments can either be physical measurements made of an object or numerical measurements using analytical models of the control volumes under study. For simplicity let us examine the simplest system, the coupling of two control volumes.

$$\begin{bmatrix}\Pi_1\\ \Pi_2\end{bmatrix} = \omega\begin{bmatrix}\eta_{11} & -\eta_{12}\\ -\eta_{21} & \eta_{22}\end{bmatrix}\begin{bmatrix}E_1\\ E_2\end{bmatrix}$$

A process to determine the loss factor is to inject power into each subsystem and measure the response on each subsystem. Define E_{rs} as the energy in system r when input power is being applied to system s to ease the notation. This leads to four equations and four unknowns for the damping and coupling loss factors –

$$\begin{aligned}\Pi_1 &= \omega\eta_1 E_{11} + \omega\eta_{12}E_{11} - \omega\eta_{21}E_{21}\\ 0 &= \omega\eta_2 E_{21} + \omega\eta_{21}E_{21} - \omega\eta_{12}E_{11}\\ \Pi_2 &= \omega\eta_2 E_{22} + \omega\eta_{21}E_{22} - \omega\eta_{12}E_{12}\\ 0 &= \omega\eta_1 E_{12} + \omega\eta_{12}E_{12} - \omega\eta_{21}E_{22}\end{aligned}$$

The coupling loss factors can be written as

$$\eta_{21} = \frac{\frac{\Pi_1}{\omega E_{11}}}{\left(\frac{E_{22}}{E_{12}} - \frac{E_{21}}{E_{11}}\right)} \qquad \eta_{12} = \frac{\frac{\Pi_2}{\omega E_{22}}}{\left(\frac{E_{11}}{E_{21}} - \frac{E_{12}}{E_{22}}\right)}$$

Note the coupling loss factors are not reciprocal, $\eta_{12} \neq \eta_{21}$.

The damping loss factors can be written as

$$\eta_1 = \frac{\Pi_1}{\omega E_{11}}\left[\frac{1-\frac{\Pi_2}{\Pi_1}\left(\frac{E_{21}}{E_{22}}\right)}{\left(1-\frac{E_{12}}{E_{22}}\frac{E_{21}}{E_{11}}\right)}\right] \qquad \eta_2 = \frac{\Pi_2}{\omega E_{22}}\left[\frac{1-\frac{\Pi_1}{\Pi_2}\left(\frac{E_{12}}{E_{11}}\right)}{\left(1-\frac{E_{21}}{E_{11}}\frac{E_{12}}{E_{22}}\right)}\right]$$

At this point we have proposed a way of expressing power balance using a coupling loss factor and have demonstrated that the coupling loss factors can be computed from the measurement of control volume energies. It should be clear on examining the equations that the values of the coupling loss factors will be a function of the definition of energy used in their calculation. From the perspective of the measurement of energy in a structure, the kinetic energy is relatively easy to measure using accelerometers or other motion-detecting systems such as laser interferometers, etc. In the acoustic field, the sound pressure level or potential energy is a more accessible measurement quantity.

In statistical energy analysis we are interested in the resonant energy in a control volume. One feature of resonant energy is that it is equally divided between kinetic and potential energy over one cycle of motion. The statistical energy analysis coupling loss factors are based on the coupling of the resonant energy in the control volumes.

The power balance equations, as shown, are very general as is the definition of the coupling loss factor. Having a measurement method is good but for a predictive scheme an estimating procedure for the coupling loss factors is needed. Limiting the SEA coupling loss factors to resonant energy exchanges and the control volumes to subsystems with high modal overlaps leads to useful and simple coupling loss factor estimating techniques based on the impedances of infinite systems. SV

The author can be contacted at evan.b.davis@boeing.com.